SPRINGER BRIEFS IN PHYSICS

Zeev Zalevsky Editor

Super-Resolved Imaging

Geometrical and Diffraction Approaches

Springer

SpringerBriefs in Physics

For further volumes:
http://www.springer.com/series/8902

Zeev Zalevsky
Editor

Super-Resolved Imaging

Geometrical and Diffraction Approaches

Springer

Editor
Zeev Zalevsky
School of Engineering
Bar-Ilan University
Ramat-Gan 52900, Israel
zalevsz@macs.biu.ac.il

ISSN 2191-5423 e-ISSN 2191-5431
ISBN 978-1-4614-0832-1 e-ISBN 978-1-4614-0833-8
DOI 10.1007/978-1-4614-0833-8
Springer New York Dordrecht Heidelberg London

Library of Congress Control Number: 2011934035

Printed on acid-free paper

Springer is part of Springer Science+Business Media (www.springer.com)

Preface

Super resolution is one of the most fascinating and applicable fields in optical data processing. The urge to obtain highly resolved images using low-quality imaging optics and detectors is very appealing.

The field of super resolution may be categorized into two groups: diffractive and geometrical super resolution. The first deals with overcoming the resolution limits that are dictated by diffraction laws and related to the numerical aperture of the imaging lens. The second deals with overcoming the limitation determined by the geometrical structure of the detector array.

Various techniques have been developed to deal with both types of resolution improvements. In all approaches, the spatial resolution improvement needs the object to exhibit some sort of constraint (such as monochromaticity, slow variation with time, single polarization, etc.), related with an unused dimension of the object. The improvement is thus made at the price of sacrificing unused degrees of freedom in the other domains as time, wavelength, polarization, or field of view.

The methods pursuing super resolution utilize masks having diffractive features. They are classified here according to the nature of their structure:

1. Possessing full/piecewise periodicity
2. Spatially finite repeating random structures/random structure with finite period
3. Random structure with infinite period

The book is thus organized in the following way. Chapter 1 briefly presents the relevant theoretical background. Chapter 2 discusses several super resolution methods implementing diffractive masks having a certain degree of periodicity. In Chapter 3, we explore techniques utilizing diffractive masks having structures with a finite random period. Finally, in Chapter 4, the mask becomes fully random.

Ramat-Gan, Israel | Zeev Zalevsky

Contents

Contributors

Amikam Borkowski School of Engineering, Bar-Ilan University, Ramat-Gan, Israel

Javier García Departamento de Óptica, Universitat de Valencia, Burjassot, Spain

Bahram Javidi Department of Electrical and Computer Engineering, University of Connecticut, Storrs, CT, USA

David Mendlovic Department of Electrical Engineering – Physical Electronics, Faculty of Engineering, Tel-Aviv University, Ramat Aviv, Israel

Vicente Micó Departamento de Óptica, Universitat de Valencia, Burjassot, Spain

Jonathan Solomon Department of Electrical Engineering – Physical Electronics, Faculty of Engineering, Tel-Aviv University, Ramat Aviv, Israel

David Sylman School of Engineering, Bar-Ilan University, Ramat-Gan, Israel

Zeev Zalevsky School of Engineering, Bar-Ilan University, Ramat-Gan, Israel

Alex Zlotnik School of Engineering, Bar-Ilan University, Ramat-Gan, Israel

Chapter 1
Theoretical Background

Alex Zlotnik, Zeev Zalevsky, David Mendlovic, Jonathan Solomon, and Bahram Javidi

1.1 Fourier Optics

1.1.1 Free Space Propagation: Fresnel and Fraunhofer Integrals

Under scalar diffraction theory assumption and assuming that work is relatively close to optical axis $\sqrt{(x-\xi)^2+(y-\eta)^2} \ll z_0$, it is possible to write the following relationship [1]:

$$U(x,y,z_0)=\frac{\exp(jkz_0)}{j\lambda z_0}\iint U^i(\xi,\eta)\exp\left\{j\frac{\pi}{\lambda z_0}\left[(x-\xi)^2+(y-\eta)^2\right]\right\}\mathrm{d}\xi\mathrm{d}\eta. \quad (1.1)$$

This is known as the Fresnel diffraction integral. It can be calculated as a convolution between the incident field U_i and the free space propagation (FSP) quadratic phase function.

In certain limiting cases, Fresnel diffraction formula can be simplified to yield Fraunhofer diffraction integral. If the diffraction is observed on a very remote plane, the quadratic phase factor inside the integral of (1.1) can be omitted, provided that the following condition is fulfilled:

$$\frac{\pi}{\lambda z_0}\left(\xi^2+\eta^2\right)_{\max}=\pi \quad \Rightarrow \quad z_0=\frac{D^2}{\lambda}.$$

Z. Zalevsky (✉)
School of Engineering, Bar-Ilan University, Ramat-Gan, Israel
e-mail: zalevsz@macs.biu.ac.il

Z. Zalevsky (ed.), *Super-Resolved Imaging: Geometrical and Diffraction Approaches*, SpringerBriefs in Physics, DOI 10.1007/978-1-4614-0833-8_1,

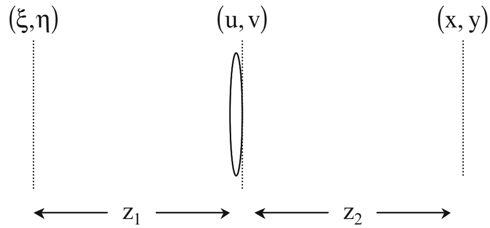

Fig. 1.1 Imaging system consists of lens with focal length *f*; (ξ, η) is the object plane, and (x, y) is the image plane

The obtained result is then:

$$U(x, y, z_0) = \frac{\exp(jkz_0)}{j\lambda z_0} \exp\left[j\frac{\pi}{\lambda z_0}\left(x^2 + y^2\right)\right] \times \iint U^i(\xi, \eta) \exp\left[-j\frac{\pi}{\lambda z_0}(x\xi + y\eta)\right] \mathrm{d}\xi \mathrm{d}\eta. \quad (1.2)$$

1.1.2 Imaging System

In this section, a simple imaging system consisting of a single thin lens of a finite aperture $P(u, v)$ and a focal length *f* is briefly analyzed. This system images a planar object in the (ξ, η) plane into a (x, y) image plane, while a monochromatic illumination is assumed (see Fig. 1.1).

1.1.2.1 Coherent Illumination

The output field $U_{\mathrm{image}}(x, y)$ is related to input $U_{\mathrm{object}}(\xi, \eta)$ through a superposition integral:

$$U_{\mathrm{image}}(x, y) = \iint U_{\mathrm{object}}(\xi, \eta) h(x, y; \xi, \eta) \mathrm{d}\xi \mathrm{d}\eta, \quad (1.3)$$

where $h(\cdot;\cdot)$ is the amplitude at image coordinates (x, y) in response to a point – source object at (ξ, η), and is given by [1]:

$$h(x, y; \xi, \eta) = \frac{1}{\lambda^2 z_1 z_2} \exp\left[i\frac{\pi}{\lambda(z_2 - f)}\left(x^2 + y^2\right)\right] \times \iint P(u, v) \exp\left\{-i\frac{2\pi}{\lambda z_2}[(x - M\xi)u + (y - M\eta)v]\right\} \mathrm{d}u \mathrm{d}v, \quad (1.4)$$

where M is the magnification, $M = -z_2/z_1$; z_1, z_2, and f obey the relation:

$$\frac{1}{z_1} + \frac{1}{z_2} = \frac{1}{f}. \tag{1.5}$$

After several simple coordinate transformations, one can obtain a convolution relationship:

$$U_{\text{image}}(x,y) = \tilde{h}(x,y) \otimes U_{\text{g}}(x,y), \tag{1.6}$$

where U_{g} is the geometrical optics prediction of the image; $\tilde{h}(x,y)$ is the point-spread function with a quadratic phase factor omitted.

1.1.2.2 Incoherent Illumination

Imaging systems using spatially incoherent illumination are linear in intensity [1] and obey the intensity convolution integral:

$$I_{\text{image}}(x,y) = \kappa \cdot |h(x,y)|^2 \otimes I_{\text{g}}(x,y), \tag{1.7}$$

where κ is a constant; $I_{\text{image}}(x, y)$ and $I_{\text{g}}(x, y)$ are intensities of $U_{\text{image}}(x, y)$ and $U_{\text{g}}(x, y)$, respectively.

1.2 Diffraction Resolution Limitation

Let us assume that we have an optical system that relies on a lens with a focal length f and aperture D. If such a system stares on a scene located at a distance of R from the sensor ($R>>f$), the viewed resolution in the image plane is limited by diffraction:

$$h(r) \propto \left| \frac{J_1(\pi r/\lambda F_{\#})}{r/\lambda F_{\#}} \right|^2 \tag{1.8}$$

and therefore equals to $1.22\lambda F_{\#}$, where r is the radial coordinate in the focal plane $r = \sqrt{x^2 + y^2}$, λ is the wavelength, and $F_{\#}$ is the F-number of the imaging system $F_{\#} = f/D$.

By translating the resolution bound to the object plane, the smallest detail possibly viewed is of the size:

$$(\delta r)_{\text{diff}} = 1.22\frac{\lambda}{D}R. \tag{1.9}$$

1.3 Geometrical Resolution Limitation

However, modern optical system are digital and contain some form of an electronic sensor. The sensor has nonzero pixels, having a size of Δd. The pixel size provides the "geometrical resolution" bound. This limitation expressed in the object plane yields:

$$(\delta x)_{\mathrm{g}} = \frac{\Delta d}{f} R. \tag{1.10}$$

In most cases, $\Delta d > 1.22(\lambda f/D)$, and the geometrical resolution is the bottleneck, in the optical system.

1.3.1 The Effects of Sampling by CCD (Pixel Shape and Aliasing)

Let us assume that an image is received on the CCD plane. The CCD samples the image with finite pixels having a defined pitch. Let us denote the distance between each pixel as Δx and the width of each pixel as Δd. Sampling the image creates replicas of the continuous image spectrum in the frequency domain. These replicas are spaced at a constant offset in the spectrum, which is proportional to the resolution of the CCD, $\Delta \nu = 1/\Delta x$.

Therefore, sampling the physical image by the CCD is equivalent to [2]:

(a) Convolving it with a rect function (a rectangular window) with a width equal to the size of a single CCD pixel. The latter simulates the effect of the nonzero pixel size.
(b) Multiplying the input by a comb function $\sum_m \delta(x - m\Delta x)$.

In the frequency plane, this is equivalent to:

(a) Multiplying the original's input spectrum by a sinc function $(\sin c(x) = (\sin(\pi x)/\pi x))$ with a width of $2/\Delta d$
(b) Convolving the result with a train of Dirac functions (due to the pixel spacing) $\sum_n \delta(\nu - (n/\Delta x))$

If the distance between the replicas is not sufficient, the replicas overlap. As a result, the image is corrupted. Figure 1.2a presents an input spectrum, and the aliased corrupted spectrum is shown in Fig. 1.2b.

Aliasing occurs when the image's resolution is more than half of that of the CCD (Nyquist sampling rate). Image resolution measured on the CCD plane is denoted as $\Delta \nu_{\mathrm{image}}$. In mathematical terms, aliasing occurs when $2\Delta \nu_{\mathrm{image}} > \Delta \nu$. Diffraction effects have been neglected as it is assumed that geometrical resolution bound is dominant.

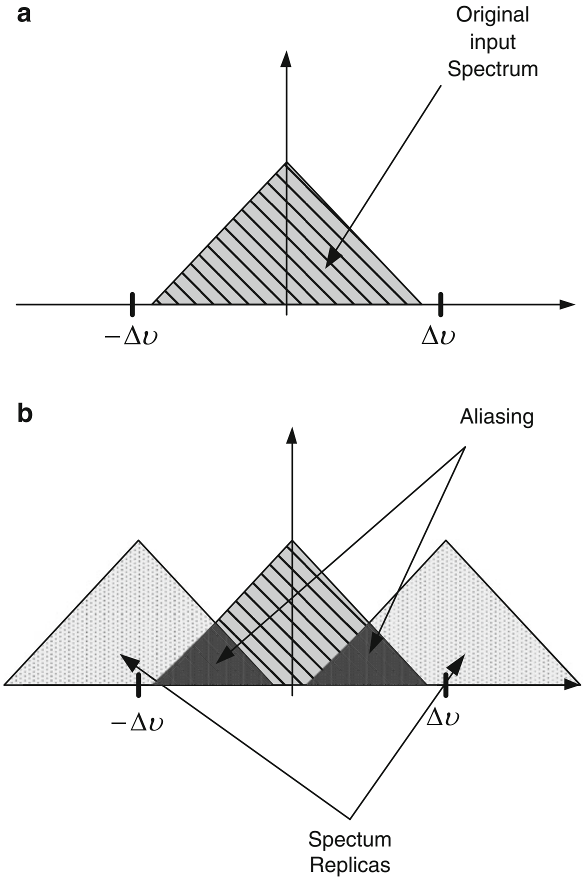

Fig. 1.2 (**a**) Output image spectrum before being sampled by CCD. (**b**) Output image spectrum after being sampled by CCD. The image was taken from: J. Solomon, Z. Zalevsky and D. Mendlovic, "Geometrical Super Resolution by Code Division Multiplexing," Appl. Opt. 44, 32–40 (2005)

1.4 Super Resolution Explained by Degrees of Freedom Number

The possibility for super resolution is often explained by the notion of degrees of freedom (DoF) invariance of a given optical system. Other term describing the same is the information capacity of the optical system. That is the number of degrees of freedom (DoF) number the system could pass through is constant and equal to information capacity [3]:

$$N = (1 + 2L_xB_x)(1 + 2L_yB_y)(1 + 2L_zB_z) \times (1 + 2L_\mathrm{T}B_\mathrm{T})\log(1 + \mathrm{SNR}), \tag{1.11}$$

where L_x L_y is the field of view, L_z is the depth of field, B_x B_y B_z is the spatial bandwidth in x, y, z dimensions; L_T is the observation interval and B_T is the temporal bandwidth. SNR is the signal-to-noise ratio. A priori knowledge of object properties makes possible to code the object in order to pass it through optical system inferior in certain DoF and superior in others. An example for such coding is

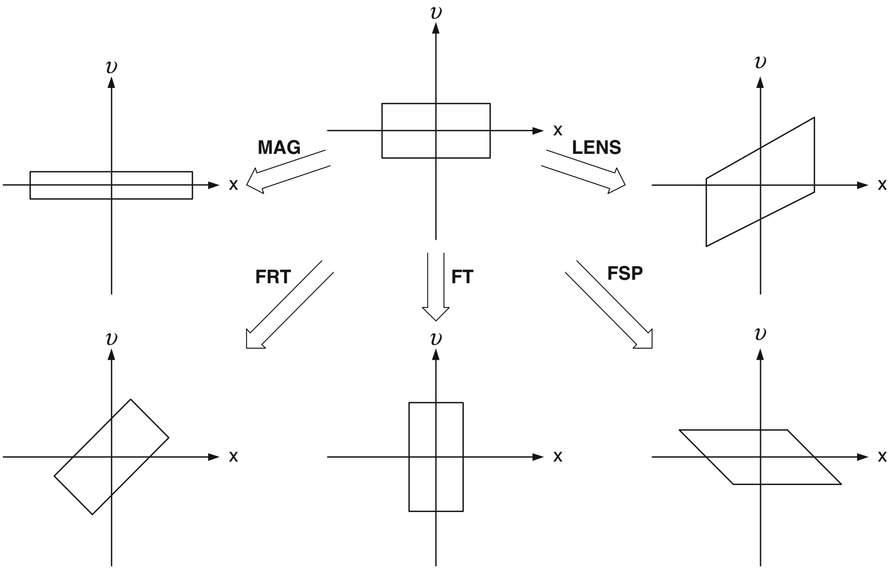

Fig. 1.3 Wigner properties

object space bandwidth (SW) shaping in Wigner space [4]. Space bandwidth product is the lateral DoF from (1.11). For 1-D signal, it is defined as

$$\mathrm{SW} = \Delta x \Delta v, \tag{1.12}$$

Δx is the area where the signal $u(x)$ is essentially nonzero and $\Delta \upsilon$ is the size of the frequency where the spectrum of $u(x)$ is essentially nonzero.

1.4.1 Wigner Transform

A Wigner chart is a wave-optical generalization of the Delano diagram (ray optics $Y\bar{Y}$ diagram). Its definition is:

$$W(x, v) = \int_{-\infty}^{\infty} u\left(x + \frac{x'}{2}\right) u^* \left(x - \frac{x'}{2}\right) \exp(-2\pi i v x') \mathrm{d}x', \tag{1.13}$$

where $u(x)$ is the complex amplitude and v is the spatial frequency. Apparently, a Wigner chart presents the spatial and spectral information simultaneously. It doubles the number of dimensions; thus, a one-dimensional (1-D) object has a two-dimensional (2-D) Wigner chart. Figure 1.3 shows the effects of elementary optical modules, such as magnification (MAG), a lens (LENS), FSP, and Fourier transform (FT) or fractional Fourier transform (FRT), on the Wigner chart of a signal [5–8].

The definition of SW was generalized by the use of the ensemble average of the Wigner chart that is due to a set of signals that may enter the optical system. There instead of being a pure number, $\mathrm{SW}(x, v)$ was a binary function of two variables (referring to as 1-D object) with the following definition:

$$\mathrm{SW_B}(x, \upsilon) = \begin{cases} 1 & f\langle W(x, v)\rangle > W_{\text{thresh}}, \\ 0 & \text{otherwise.} \end{cases} \quad (1.14)$$

The area of $\lim_{x\to\infty} \mathrm{SW}(x, v)$ indicates in fact the number of DoF; e.g., if δx denotes the spatial resolution and δv is the spectral resolution, then $\delta x = 1/\Delta v$, $\delta v = 1/\Delta x$, and the number of degrees of freedom (DoF) N is:

$$N = \frac{\Delta x}{\Delta \delta} = \frac{\Delta v}{\delta v} = \Delta x \cdot \Delta v. \quad (1.15)$$

For a given optical system whose SW acceptance capabilities are denoted by $\mathrm{SWY}_\upsilon(x, v)$ and a given input signal whose existing SW is denoted by $\mathrm{SWI}_\upsilon(x, v)$, a necessary condition for transmitting the whole signal without information loss is:

$$\mathrm{SWI}_v(x, v) \subseteq \mathrm{SWY}_v(x, v). \quad (1.16)$$

If the transmission is lossless, then the following condition takes place:

$$N_{\text{signal}} \leq N_{\text{system}}. \quad (1.17)$$

1.5 Inverse Problem Statement of Super Resolution

Achieving either geometrical or diffraction super resolution can be formulated as solving inverse problem.

Inverse problem is stated in the following manner: An image is known on a certain grid. One wishes to restore image values on a finer grid. The image is related to high-resolution unknown object through blurring, sampling, and addition of noise. The blurring is assumed to be a spatially invariant operator. It is possible to write the following discrete relationship (on a fine grid):

$$y[m,n] = g[m,n] * u[m,n] = \sum_{k=0}^{R-1} \sum_{l-0}^{R-1} g[k+m, l+n]u[k,l], \quad (1.18)$$

where $g[\ldots]$ is the blurring matrix, $u[\ldots]$ is the high-resolution object to be restored.

It is convenient to represent 2-D images as column-wise concatenated vectors and the blurring operator as a matrix. The original and blurred images are therefore assumed to be related by a compact set of linear equations:

$$\underline{\underline{A}}\underline{x} = \underline{b}. \quad (1.19)$$

In order to be defined as well-posed and to have a unique solution, it must uphold the following three conditions: existence, stability, and uniqueness [9]. If some of the conditions do not hold, then the problem is ill-posed, and there may not be a solution, or it may not be unique. Furthermore, since this solution does not uphold all three conditions mentioned above, the additive noise prevent us from converging to real solution. Likewise, since there are more unknowns than equations, the solution is not unique. Finally, a small change in one of the variables would affect the solution of the problem so that the stability of the solution would be very low.

One possible direction for the above-mentioned problems is to use the pseudoinverse matrix that is obtained by a reduction of the least square error. Techniques dealing with least square error reduction [10] involve recursive least square error (RLS) [11] and recursive total least square error (RTLS) [12]. A more sophisticated method to reduce least square errors recursively uses regularization [13]. This method which succeeds to overcome noise contains Tikhonov's regularization component. This component is designed such that for problems without noise it will be possible to reduce it so that the real solution will be approached, while for images with noise this positive addition will yet yield an optimal solution [14].

There is a set of other regularization methods that uses prior knowledge of the system regarding the statistical properties of the blurring problem. This set of methods is called stochastic reconstruction methods. In this set of methods, reconstruction of a super resolution image is a statistical re-evaluation problem, where all quantities are modeled by their probability functions. One way to reconstruct is by applying the maximum a posteriori (MAP) where the super resolved image may be obtained by looking for the maximum of the conditional probability distribution whose estimation is done by the Markov random field (MRF) in different ways, enabling the addition of a priori constraints into the solution [15, 16]. Another solution known as maximum likelihood (ML) is actually a particular case of MAP, where the required image is obtained by the ML estimator which does not need any a priori knowledge [17].

A different approach named projection onto convex sets (POCS) assumes a number of prior demands of the required solution. For each such demand, an operator is defined that projects a dot in the field of the super resolution image onto a field fulfilling the constraint. Such an iterative process of operator activation causes the solution to converge fulfilling all the constraints and even may avoid guessing the first solution either by using the time domain [18] or by using the frequency domain [19]. Following that another interesting direction for solving the blurring problem by iteration is via using the iterated back-projection (IBP) method [20].

References

1. Goodman, J.W.: Introduction to Fourier Optics, Chap. 3, 2nd edn. McGray-Hill, New York (1996)
2. Oppenheim, A.V., Willsky, A.S., Hamid, S.: Signals and Systems, Chap. 7, 2nd edn. Prentice-Hall, London (1996).
3. Cox, I.J., Shappard, C.J.R.: Information capacity and resolution in an optical system. J. Opt. Soc. Am. A **3**, 1152–1158 (1986)
4. Lohmann, A.W., Dorsch, R.G., Mendlovic, D., Zalevsky, Z., Ferreira, C.: Space-bandwidth product of optical signals and systems. J. Opt. Soc. Am. A **13**(3), 470–473 (1996)
5. Zalevsky, Z., Mendelovic, D., Lohmann, A.W.: Understanding superresolution in Wigner space. J. Opt. Soc. Am. **17**(12), 2422–2430 (2000)
6. Mendelovic, D., Lohmann, A.W.: Space-bandwidth product adaptation and its application to superresolution: fundamentals. J. Opt. Soc. Am. A **14**, 558–562 (1997)
7. Mendelovic, D., Lohmann, A.W., Zalevsky, Z.: Space-bandwidth product adaptation and its application to superresolution: examples. J. Opt. Soc. Am. A **14**, 563–567 (1997)
8. Lohmann, A.W.: Image rotation, Wigner rotation and the fractional Fourier transform. J. Opt. Soc. Am. A **10**, 2181–2186 (1993)
9. Hadamard, J.: Lectures on Cauchy's Problem in Linear Partial Differential Equation. Dover, New York (1923)
10. Tekalp, A.M., Ozkan, M.K., Sezan, M.I.: High-resolution image reconstruction from lower-resolution image sequences and space varying image restoration. In: Proceedings of the IEEE International Conference on Acoustics, Speech and Signal Processing (ICASSP), vol. 3, pp. 169–172 (1992)
11. Kim, S.P., Bose, N.K., Valenzuela, H.M.: Recursive reconstruction of high resolution image from noisy undersampled multiframes. IEEE Trans. Acoust. Speech Signal. Process. **38**(6), 1013–1027 (1990)
12. Bose, N.K., Kim, H.C., Valenzuela, H.M.: Recursive total least squares algorithm for image reconstruction from noisy, undersampled frames. Multidim. Syst. Signal Process. **4**(3), 253–268 (1993)
13. Kim, S.P., Su, W.Y.: Recursive high-resolution reconstruction of blurred multiframe images. IEEE Trans. Image Process. **2**(4), 534–539 (1993)
14. Tikhonov, A., Arsenin, V.Y.: Solutions of Ill-posed Problems. V.H Winston and Sons, Washington, DC (1977)
15. Cheeseman, P., Kanefsky, B., Kraft, R., Stutz, J., Hanson, R.: Super-resolved surface reconstruction from multiple images. In: Heidbreder, G.R. (ed.) Maximum Entropy and Bayesian Methods, pp. 293–308. Kluwer Academic Publishers, Dordrecht, The Netherlands (1996)
16. Hardie, R.C., Barnard, K.J., Armstrong, E.E.: Joint MAP registration and high-resolution image estimation using a sequence of undersampled images. IEEE Trans. Image Process. **6**(12), 1621–1633 (1997)
17. Tom, B.C., Katsaggelos, A.K.: Reconstruction of a high-resolution image from multiple-degraded misregistered low-resolution images. Vis. Commun. Image Process. SPIE **2308**(2), 971–981 (1994)
18. Stark, H., Oskoui, P.: High-resolution image recovery from image-plane arrays using convex projections. J. Opt. Soc. Am. **A6**, 1715–1726 (1989)
19. Wheeler, F.W., Hoctor, R.T., Barrett, E.B.: Super-resolution image synthesis using projections onto convex sets in the frequency domain. In: IS&T/SPIE Symposium on Electronic Imaging, Conference on Computational Imaging, vol. 5674, pp. 479–490 (2005)
20. Irani, M., Peleg, S.: Motion analysis for image enhancement: resolution, occlusion, and transparency. J. Vis. Commun. Image R. **4**(4), 324–335 (1993)